# Synthetic VSP seismograms with attenuation

Linping Dong and Gary F. Margrave

## ABSTRACT

Zero-offset synthetic VSP seismograms are created for a horizontally layered medium with constant-Q attenuation. These synthetic data are verified by the reflectivity from sonic and density log and also compared to the deconvolved real VSP data recording in the well from which the log data are measured. The synthetic upgoing waves are comparable to the real upgoing waves.

## INTRODUCTION

Real VSP data always show the property of the attenuation. Many researchers have tried to generate the synthetic VSP seismograms including attenuation (Ganley, 1981; Ursin and Arntsen, 1985; Aminzadeh and Mendel, 1985; Suprajitno and Greenhalgh, 1986). Some software such as GXII also has a function to generate synthetic VSP data including attenuation. But no one provides an approach to create a synthetic VSP seismogram directly from log data, which is more useful in both VSP and surface seismic data interpretation. Accurate zero-offset VSP synthetic seismograms can connect the log data and surface seismic data together, and identify the interface corresponding to a specified reflection event in the surface data. After including attenuation, the synthetic seismograms are closer to the real data than those without attenuation. The method presented here is based upon the wavefield extrapolation theory and is applicable to plane waves in a flat layered model with constant-Q attenuation. The Q value can vary with depth but is constant within each layer.

## EXTRAPOLATION OF DOWNGOING AND UPGOING WAVES

Consider a one-dimension (1-D) layered earth with attenuation, the pressure potentials for vertically propagating plane waves at a depth level z can expressed by

$$s(z,\omega) = D(\omega)\exp\left(-\frac{\omega|z|}{2Q(z)v_H(\omega)}\right)\exp\left(-i\frac{\omega z}{v_H(\omega)}\right)$$

$$+U(\omega)\exp\left(-\frac{\omega|z|}{2Q(z)v_H(\omega)}\right)\exp\left(i\frac{\omega z}{v_H(\omega)}\right) \tag{1}$$

where $D$ and $U$ represent the downgoing and upgoing waves. $Q$ is a given frequency-independent quality factor and $v_H$ is phase velocity that can be written as

$$v_H(\omega) = v_{ref}(z)\left(1 + \frac{1}{\pi Q(z)}\ln\left|\frac{\omega}{\omega_{ref}}\right|\right) \tag{2}$$

where $v_{ref}$ is reference velocity at reference frequency $\omega_{ref}$ which is usually chosen as Nyquist frequency.

The extrapolators for downgoing and upgoing waves can be derived from Equation (1) as

$$D\left(z+\Delta z,\omega\right)=D\left(z,\omega\right)\exp\left(-\frac{\omega\left|\Delta z\right|}{2Q(z)v_H\left(z,\omega\right)}\right)\exp\left(-i\frac{\omega\Delta z}{v_H\left(z,\omega\right)}\right) \qquad (3)$$

and

$$U\left(z+\Delta z,\omega\right)=U\left(z,\omega\right)\exp\left(-\frac{\omega\left|\Delta z\right|}{2Q(z)v_H\left(z,\omega\right)}\right)\exp\left(i\frac{\omega\left|\Delta z\right|}{v_H\left(z,\omega\right)}\right) \qquad (4)$$

where $\Delta z > 0$ for downgoing waves and $\Delta z < 0$ for upgoing waves.
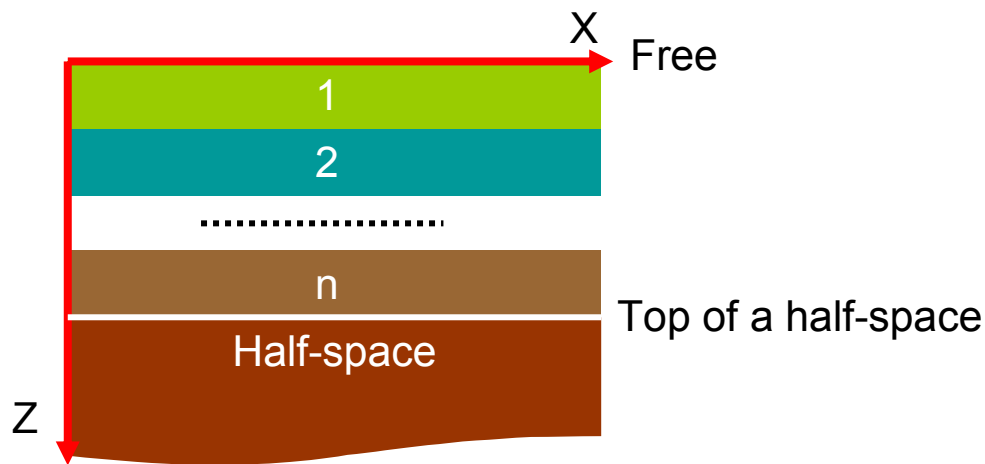


FIG. 1. *n* horizontal layers over a half-space.

For the vertical-incidence VSP in *n* layers over a half-space as shown in Figure 1, the effect of reflection/transmission should be included in the wavefield extrapolation. Suppose the thickness of *j*th layer is $h_j$ and the step of the extrapolation is equal to $h_j$. The relation between the wavefield just beneath the *j*th interface and those immediately under the *j*-1th interface (as shown in Figure. 2) can be derived as

$$D'\left(z+h_j,\omega\right)=T_jD\left(z,\omega\right)e^{-\frac{\omega h_j}{2Q(j)v_H(j,\omega)}}e^{-\frac{\omega h_j}{v_H(j,\omega)}}+R_j'U\left(z,\omega\right)e^{-\frac{\omega h_j}{2Q(j)v_H(j,\omega)}}e^{\frac{\omega h_j}{v_H(j,\omega)}}, \quad (5)$$

and

$$U'\left(z+h_j,\omega\right)=\frac{R_j}{T_j'}D\left(z,\omega\right)e^{-\frac{\omega h_j}{2Q(j)v_H(j,\omega)}}e^{-\frac{\omega h_j}{v_H(j,\omega)}}+\frac{1}{T_j'}U\left(z,\omega\right)e^{-\frac{\omega h_j}{2Q(j)v_H(j,\omega)}}e^{\frac{\omega h_j}{v_H(j,\omega)}}, \quad (6)$$

where $R_j$ and $T_j$ are complex reflection and transmission coefficients at the jth interface as seen from above, and $R_j'$ and $T_j'$ are the corresponding coefficients of the jth surface seen from below. The reflection coefficient $R_j$ is written as (Ganley, 1981)

$$R_j = \frac{\rho_{j+1}v_{Cj+1} - \rho_j v_{Cj}}{\rho_{j+1}v_{Cj+1} + \rho_j v_{Cj}} \qquad (7)$$

and the other three coefficients can be easily derived from $R_j$. $v_{Cj}$ is complex velocity which relates to phase velocity by (Aki and Richard, 1980)

$$\frac{1}{v_{Cj}} = \frac{1}{v_{Hj}}\left(1 + \frac{i}{2Q(j)}\right) \qquad (8)$$
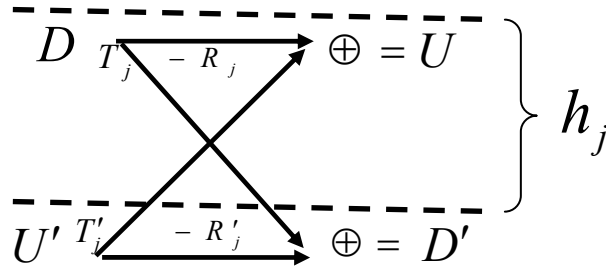


FIG. 2. Relation of incidence, reflection and transmission waves on a subsurface.

The boundary conditions are necessary for wavefield extrapolation. As shown in Figure 1, we assume the top boundary is free surface and the bottom is top of a half-space. The input is the Fourier spectrum of the downgoing source signature at the surface, denoted by $s(\omega)$. Then the total downgoing waves in the top layer will be made up of this spectrum plus the reflection of the upgoing wave off the surface. That is

$$D(h_1,\omega) = s(\omega) - R_0 U(h_1,\omega), \qquad (9)$$

where $R_0$ is the reflection coefficient as seen from above. Equations (5) and (6) can also be written as

$$\begin{pmatrix} D'(z+h_j) \\ U'(z+h_j) \end{pmatrix} \begin{pmatrix} T_j e^{-\frac{\omega h_j}{2Q(j)v_H(j,\omega)}} e^{-\frac{\omega h_j}{v_H(j,\omega)}} R'_j e^{-\frac{\omega h_j}{2Q(j)v_H(j,\omega)}} e^{\frac{\omega h_j}{v_H(j,\omega)}} \\ \frac{R_j}{T'_j} e^{-\frac{\omega h_j}{2Q(j)v_H(j,\omega)}} e^{-\frac{\omega h_j}{v_H(j,\omega)}} \frac{1}{T'_j} e^{-\frac{\omega h_j}{2Q(j)v_H(j,\omega)}} e^{\frac{\omega h_j}{v_H(j,\omega)}} \end{pmatrix} \begin{pmatrix} D(z) \\ U(z) \end{pmatrix} = A_j \begin{pmatrix} D(z) \\ U(z) \end{pmatrix} (10)$$

where $A_j$ is only related to the model parameters. From equation (10), the wavefield in the first layer and that just below the top the half-space are related by

$$\begin{pmatrix} D'(z+h_n) \\ U'(z+h_n) = 0 \end{pmatrix} = A_n \cdots A_j \cdots A_i \begin{pmatrix} D(h_1) \\ U(h_1) \end{pmatrix} = A \begin{pmatrix} D(h_1) \\ U(h_1) \end{pmatrix} \qquad (11)$$

Solving the upgoing wave in the first layer and downgoing wave in the half-space from equations (9) and (11), the waves in any layer within the model can be calculated by extrapolation from either the first layer or the half space.

## ANALYSIS OF THE SYNTHETIC SEISMOGRAMS

The model for synthetic data can be constructed from sonic and log data by making equal time layers (Margrave, 1996). Figure 3 shows the log data and impedance curve from the horizontal layers with equal traveltime of 0.002 s. Q for each layer is 50. Source signature was chosen as a minimum phase wavelet with dominant frequency of 50 Hz as shown in Figure 4.

Figure 5 shows the synthetic VSP data from the given model. These data consist of both primary downgoing and upgoing waves which are attenuated with increasing depth. Figures 6 and 7 show the downgoing waves and their amplitude spectra. The high-frequency components are attenuated much more in deep traces than in shallow traces. Figure 8 shows the given Q and Q estimates by spectral ratio method from the amplitude spectra shown in Figure 7. Q estimates are more accurate if the two traces used for Q estimation are far from each other. Figure 9 shows the impedance of the given model and the flatten upgoing waves. The reflection location in the synthetic VSP is consistent with the change in impedance. The polarity of the reflected pulses is also related to the variation in impedance. The increase in impedance corresponds to negative polarity while the decrease in impedance produces positive pulses.

In Wiener deconvolution of the upgoing waves, the deconvolution operators are designed from downgoing waves and then applied to the corresponding upgoing waves. The corridor stack of the deconvolved upgoing waves is equivalent to the nonstationary deconvolution of the reflected wave received on the surface at zero offset and comparable to the reflectivity generated from sonic and density logs. Figure. 10 shows the deconvolved traces within corridor, the corridor stack and the reflectivity. Both the corridor stack and the reflectivity are filtered by a zero-phase filter with bandpass from 10 to 125 Hz. They are consistent very well in major reflection coefficients. This also shows that the synthetic VSP data are accurate.

The real data is generated from vibration source and the equivalent source signature is shown in Figure 11. We generated synthetic data from the same source signature and compare the synthetic downgoing waves to the real downgoing waves as shown in Figure 12 and 13. The wave shape of the wavelet in the synthetic data is similar to that of the real data in both shallow and deep areas as shown in the box displayed in the Figures. After Wiener deconvolution to the upgoing waves and corridor stack, we compare the corridor stacked trace to the reflectivity from the log data. Figure 14 shows the deconvolved upgoing waves, the corridor stacked trace and bandpass-filtered reflectivity. The similarity between the stacked trace and the reflectivity shows that the wavelets embedded in the upgoing waves are close to the minimum phase. Figure. 15 shows deconvolved upgoing synthetic and real data. The main reflection events in both data are coincident. Since at present our synthetic data only include attenuated primary waves, the difference between synthetic and real data is caused by many factors such as the ground force, near-surface influence, and residual multiples.

## CONCLUSIONS

The synthetic VSP seismograms are generated and their accuracy is verified by Q estimates, impedance and reflectivity from log. VSP synthetic data are also consistent with real VSP data. The wavelet embedded in the synthetic data with attenuation approximates to minimum phase though the source signature is Klauder wavelet.

## ACKNOWLEDGEMENTS

## REFERENCES

Aki, K., and Richards, P.G., 1980, Quantitative Seismology, Theory and Methods: W.H. Freeman and Company.

Aminzadeh, F. and Mendel, J.M., 1985, Synthetic vertical seismic profiles from nonnormal incidence plane waves: Geophysics, **50**, 127-141.

Ganley, D. C., 1981,A method for calculating synthetic seismograms which include the effects of absorption and dispersion: Geophysics, **46**, 1100-1107.

Margrave, G. F., 1996, Matlab code: synth: CREWES.

Suprajitno, M. and Greenhalgh, S.A., 1986, Theoretical vertical seismic profiling seismograms: Geophysics, **51**, 1252-1265.

Ursin, B., and Arntsen, B., 1985, Computation of zero-offset vertical seismic profiles including geometrical spreading and absorption: Geophysical Prospecting, **33**, 72-96.

**FIGURES**
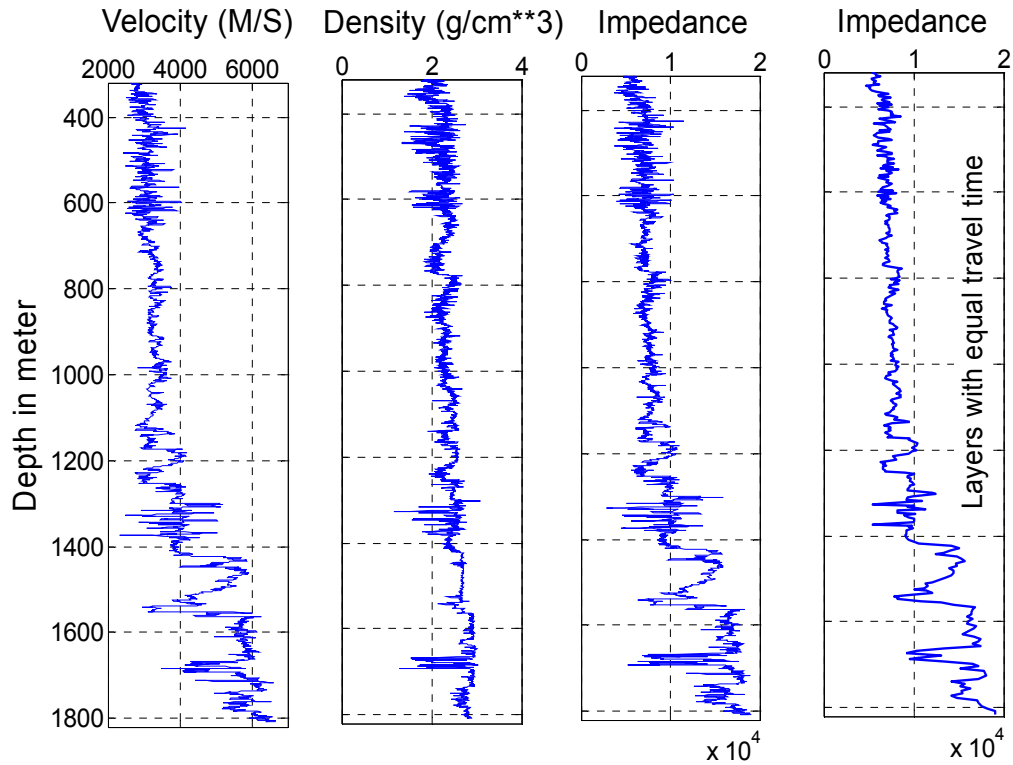


FIG. 3. Log data and impedance model consisting of the layers with equal traveltime.
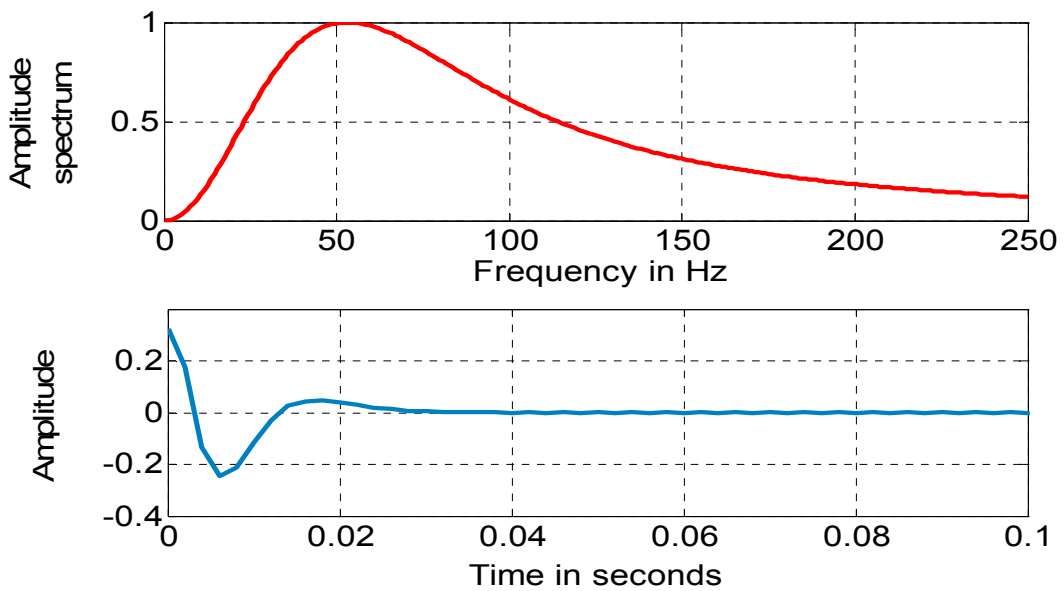


FIG. 4. Source signature and its amplitude spectrum.
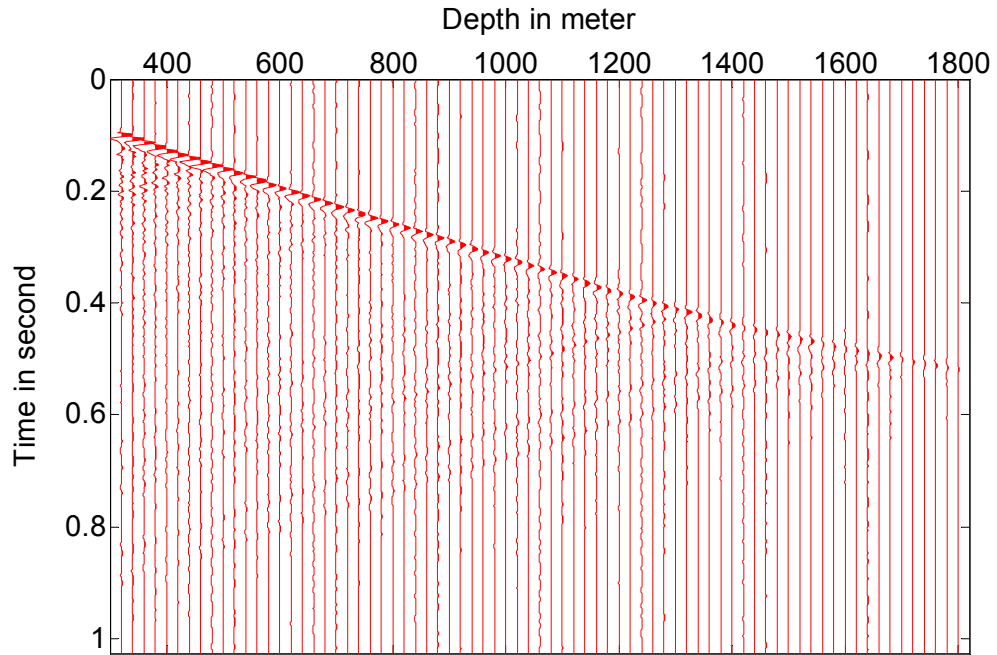
FIG. 5. Synthetic VSP seismograms including primary downgoing and upgoing waves.
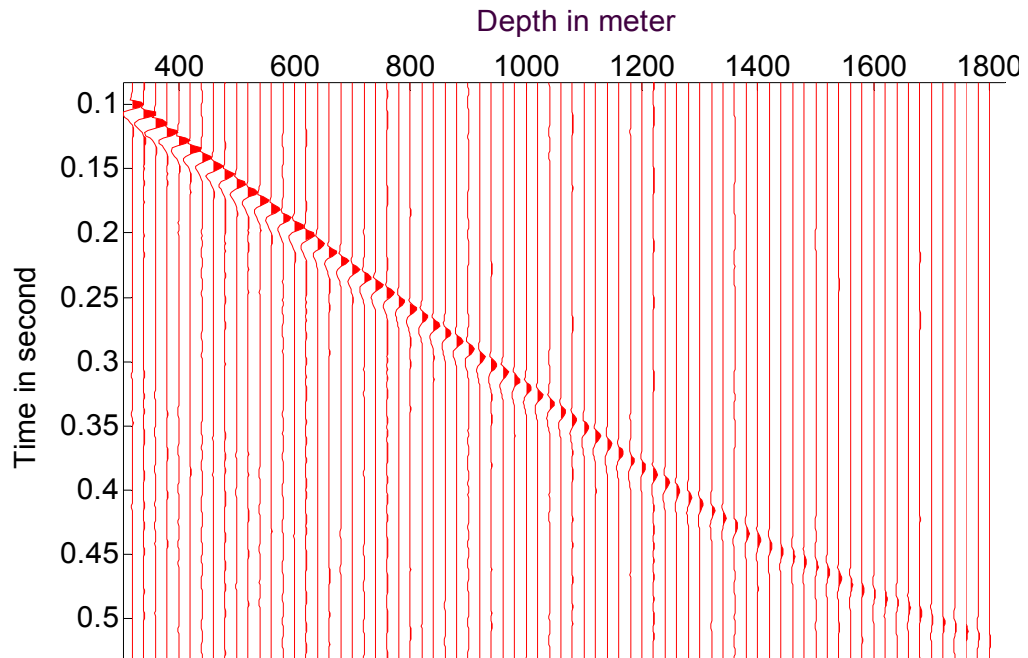


FIG. 6. Synthetic VSP downgoing waves
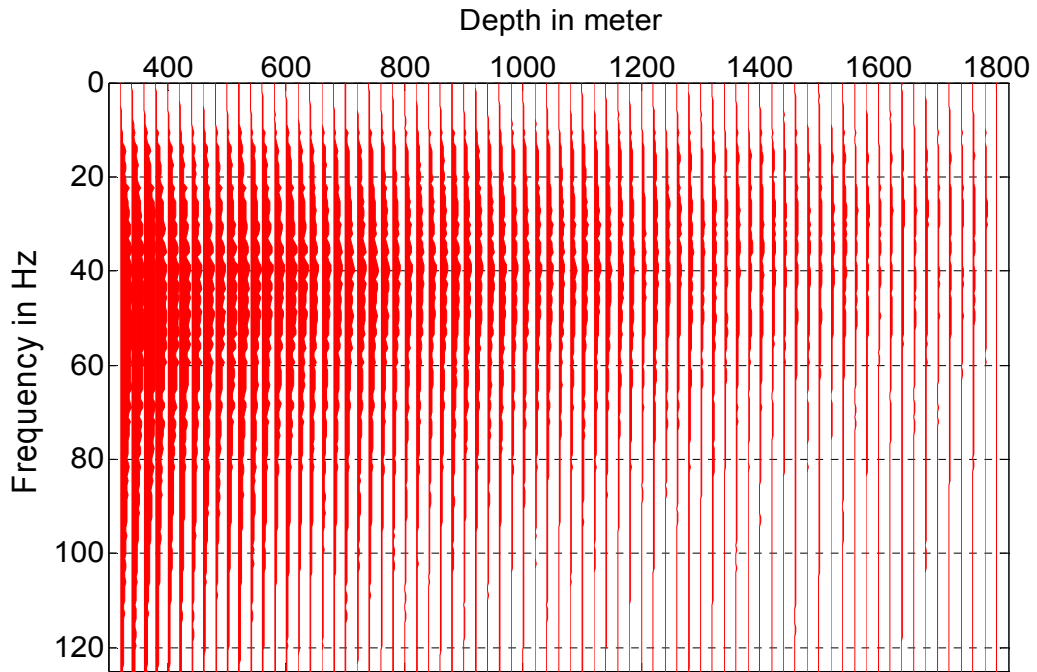
FIG. 7. Amplitude spectra of the synthetic VSP downgoing waves.
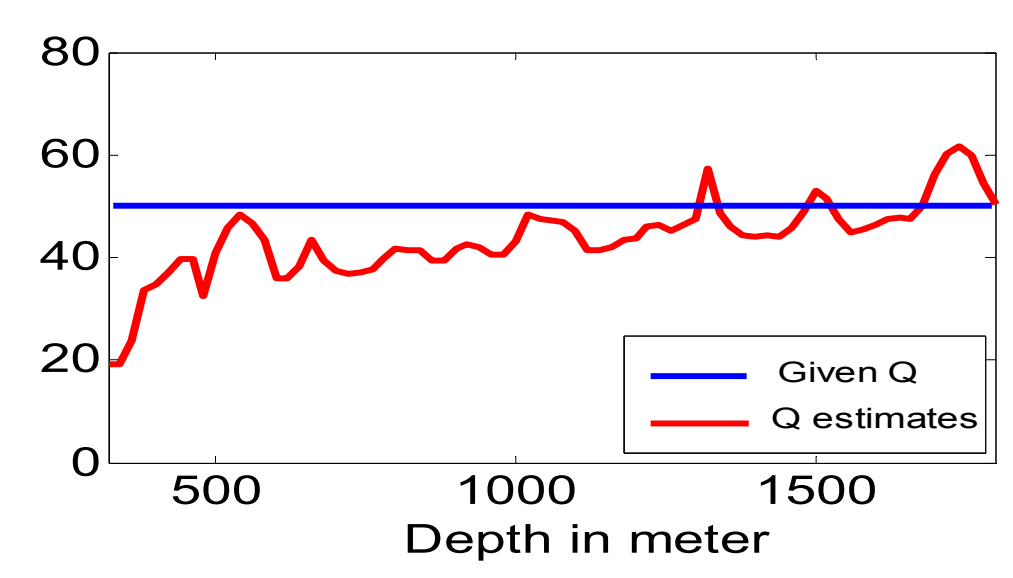


FIG. 8. Given Q and Q estimates by spectral ratio method.
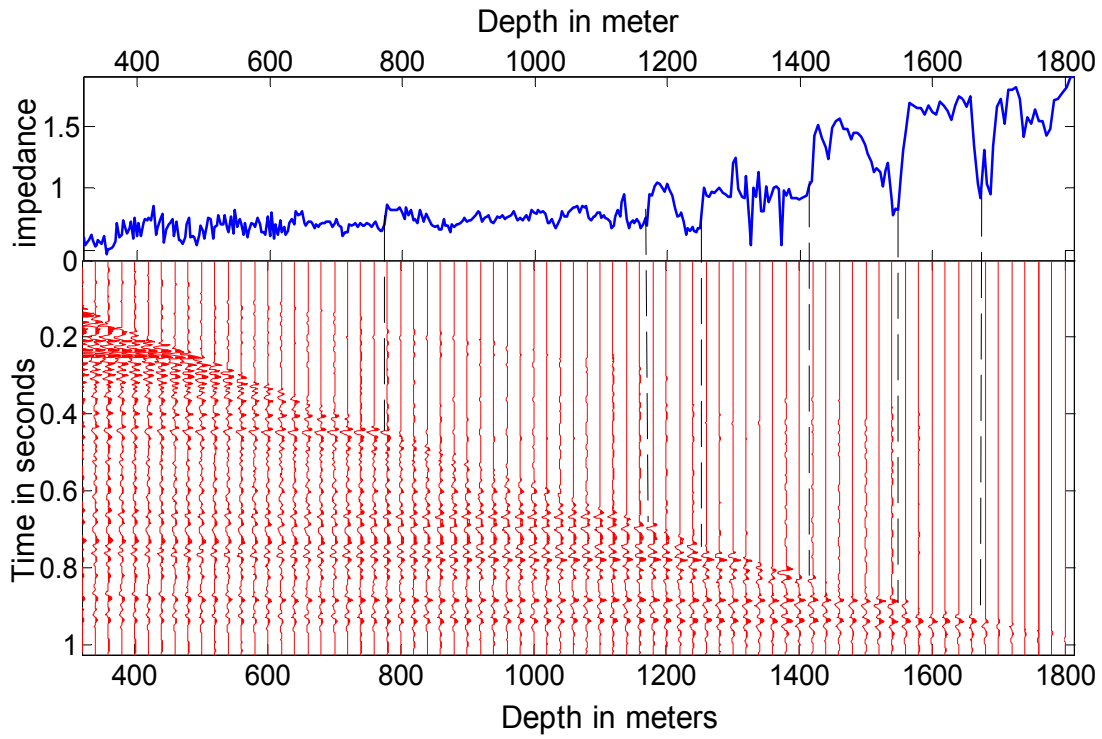
FIG. 9. Impedance and flatten synthetic upgoing waves.
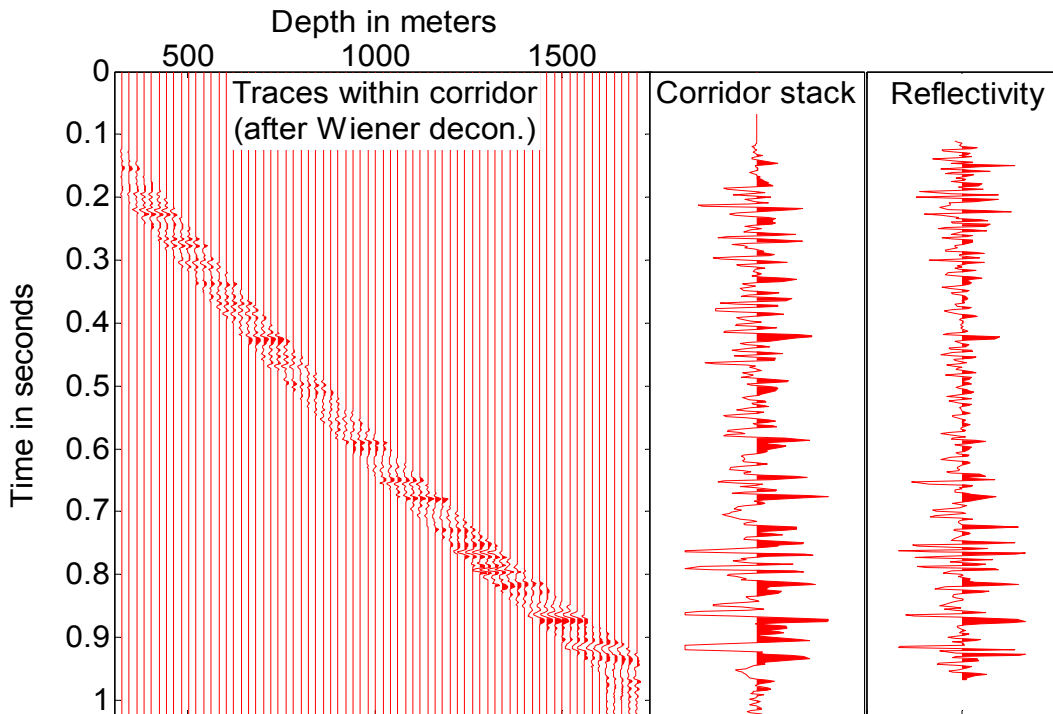
FIG. 10. Traces within the corridor, corridor stack and reflectivity.
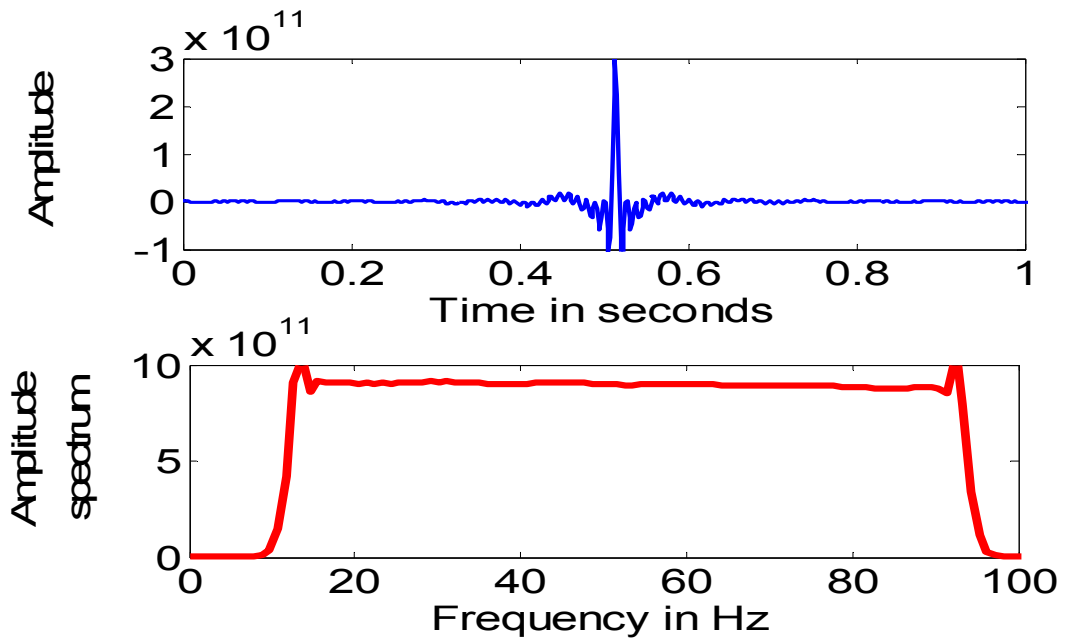
FIG. 11. Klauder wavelet and its amplitude spectrum.
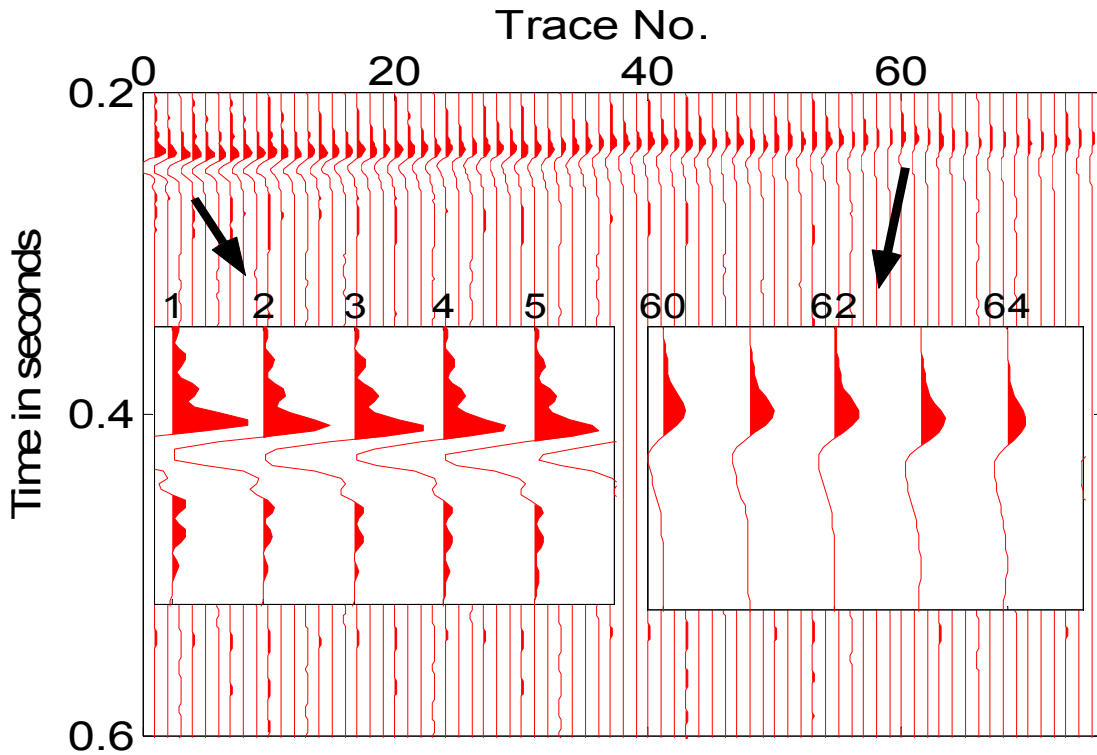


FIG. 12. Synthetic downgoing waves.
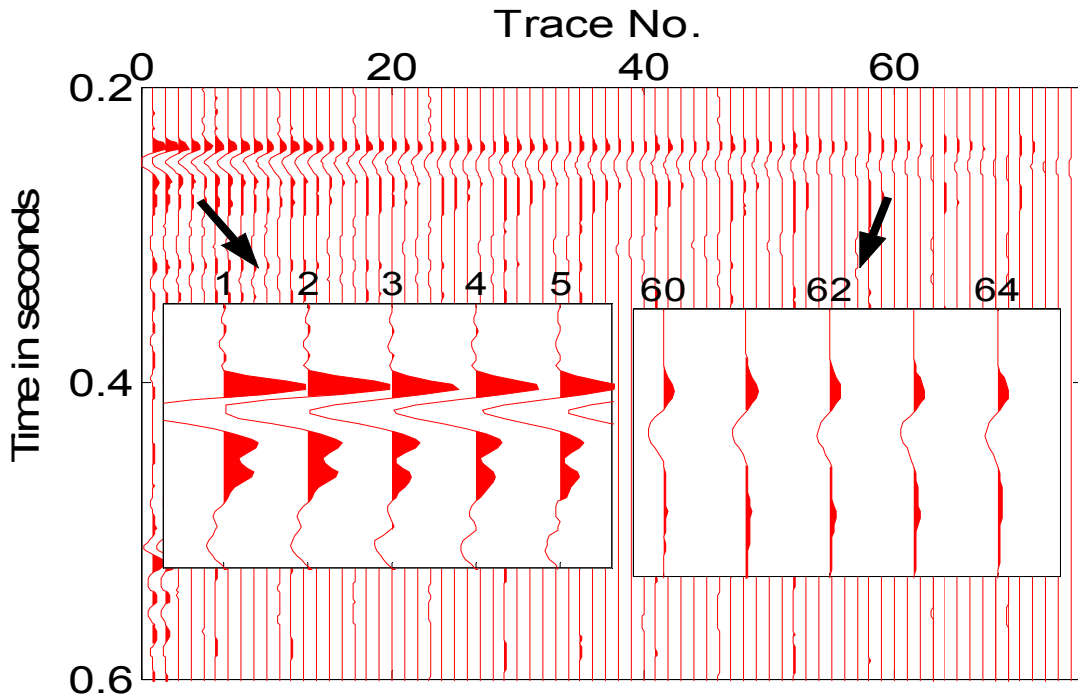
FIG. 13. Real downgoing waves.
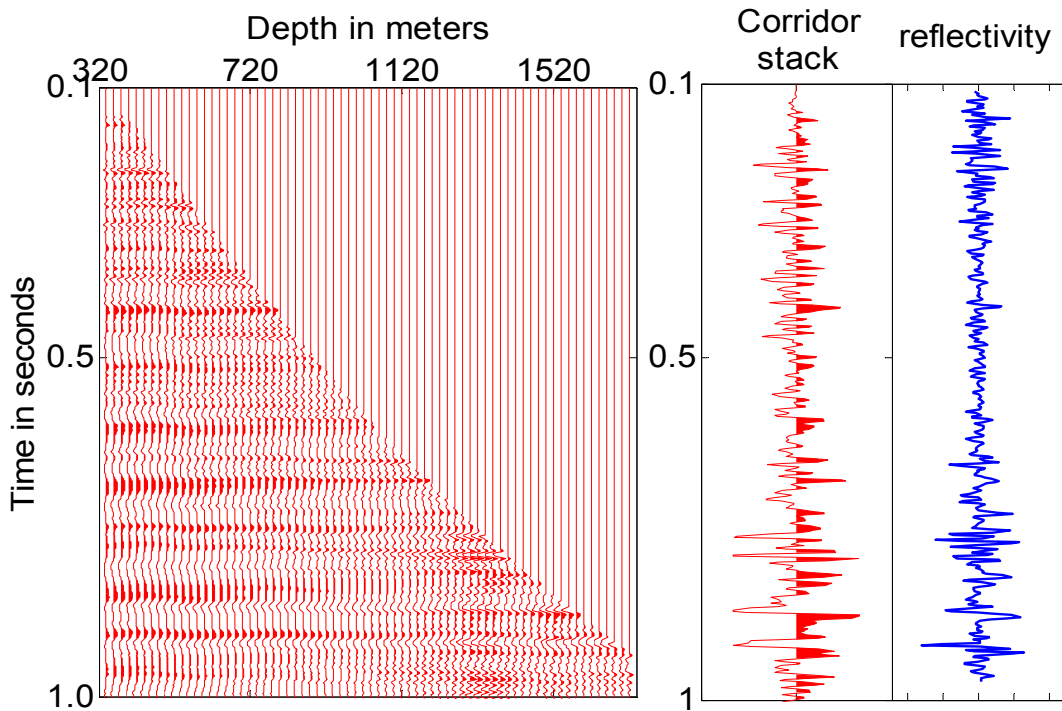


FIG. 14. Deconvolved upgoing waves, corridor stack, and reflectivity.
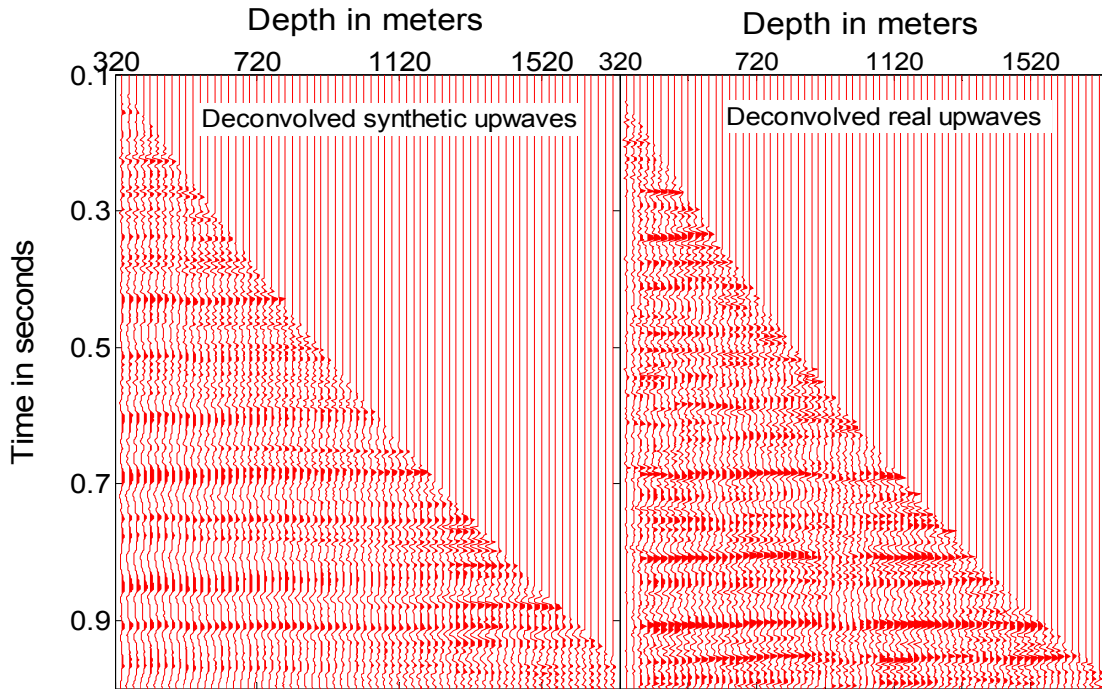
FIG. 15. Deconvolved synthetic and real upgoing waves.